Chemistry—Methods

Review
doi.org/10.1002/cmtd.202300027

Chemistry Europe
European Chemical Societies Publishing

www.chemistrymethods.org

Operando Laboratory-based X-ray Absorption Spectroscopy: Guidelines for Newcomers in the Field

Nina S. Genz,[a, b] Antti-Jussi Kallio,[c] Florian Meirer,[a] Simo Huotari,*[c] and Bert M. Weckhuysen*[a]

The new possibility to perform operando X-ray absorption spectroscopy (XAS) in the laboratory expands the potential field of applications towards a broad research community. These applications are multidisciplinary at heart and benefit from joint expertise from different fields, most importantly chemistry, physics, geology, and instrumentation. Hence, a development of collaboration networks that combine skills and knowhow from different fields is highly beneficial in this endeavor. As operando laboratory-based XAS constitutes a highly interesting, advanced, and powerful characterization technique, we provide in this article practical guidelines for newcomers in the field, who would like to employ it. Here, we will describe ten important steps towards a successful operando laboratory-based XAS experiment, which are not only useful for the catalysis community, but for a much wider audience from other research fields, such as environmental chemistry as well as battery and fuel cell research.

Introduction

X-ray absorption spectroscopy (XAS) constitutes a powerful materials characterization technique, based on measurement of the fine structure of the X-ray attenuation coefficient around a so-called X-ray absorption edge of a given element and electron shell. In the X-ray absorption process, a bound core electron can be excited into an unoccupied state above the Fermi level. X-ray absorption spectra are recorded by measuring the ratio of the transmitted and incident X-ray beam intensity, or the yield of secondary particles (such as fluorescence photons or emitted electrons) as a function of photon energy varied across the absorption edge of an element. In transmission XAS, the intensity of X-rays I after a sample with a thickness d and energy-dependent absorption coefficient μ is $I = I_0\exp(-\mu d)$, where I_0 is the incident X-ray intensity arriving on the sample. The measured quantity is the unitless absorbance μd. In the vicinity of the binding energy of an electron shell, the absorbance displays a sharp increase, that is, an increased absorption probability, which is typically called the "absorption edge". The XAS spectra give information on the average environment of the absorbing element in the sample and are commonly divided into X-ray absorption near edge structure (XANES, up to ~100 eV above the absorption threshold) and extended X-ray absorption fine structure (EXAFS, up to ~1 keV above the threshold). In XANES analysis fundamental insights into the electronic properties of the absorbing element, such as its oxidation state and the local symmetry can be obtained, while EXAFS analysis yields information on the near-neighbour bonding distances, coordination numbers, and local disorder. The main advantages, making XAS such a powerful technique, are that it is element-specific, non-destructive, and does not require long-range ordering. If using hard X-rays (> ~3 keV), it is also bulk sensitive.[1–3] For further information on the theory of XAS as well as applications of XAS for catalysis, we recommend the interested reader to dive into some valuable textbooks as well as interesting review papers,[1,2,4–18] or visit the website of the International X-ray Absorption Society (IXAS),[3] where several tutorials, introductions, and related literature recommendations are available.

The principles of XAS were discovered using conventional X-ray tubes as light sources, but with the advent of synchrotrons, XAS experiments quickly made use of the tremendous advantages given by those high-brilliance light sources. Today, XAS experiments are typically performed at a synchrotron facility.[19] Synchrotron light offers tuneable photon energy and polarization, and has further advantageous characteristics for XAS, such as high flux and small X-ray spot size, enabling high resolution both spatially and temporally. However, the continuous development of laboratory-based XAS setups nowadays offers new possibilities to perform XAS experiments also in local laboratory environments. For such laboratory-based setups, well-proven and affordable X-ray sources – high-power water-cooled ones as commonly used in X-ray diffractometers, or air-cooled lower-power sources – are routinely available from various vendors.

The landscape of XAS experiments at synchrotron versus local laboratories has been reviewed by Ditter et al.[20] Advantages of XAS at local laboratories include: 1) beamtime allocation at synchrotrons is limited, 2) access to routine analysis is more readily available at researcher's own laboratory, 3) safety considerations at synchrotron facilities render experiments with hazardous substances depreciated, 4) installation of complex sample environments for time-limited experiments is resource-costly, and 5) routine access at home laboratory also gives more possibilities for hands-on training of new users or even research purposes of students. Considering these aspects, it becomes evident that laboratory-based XAS experiments offer a clear complement and an attractive alternative to studies at a synchrotron facility.[20–31] The increasing number of publications where laboratory-based XAS has been employed to gain new insights into functional materials reflects the increasing importance of this technique, not only for ex situ,[32–44] but also for in situ studies,[30,31,45] and most recently, even for operando studies in the field of catalysis.[29] It is worth mentioning that in situ studies comprise the characterization of functional

[a] Dr. N. S. Genz, Dr. F. Meirer, Prof. Dr. B. M. Weckhuysen
Inorganic Chemistry and Catalysis group, Department of Chemistry
Utrecht University
Universiteitsweg 99, 3584 CG Utrecht, The Netherlands
E-mail: b.m.weckhuysen@uu.nl

[b] Dr. N. S. Genz
Paul Scherrer Institute
Forschungsstrasse 111, 5232 Villigen PSI, Switzerland

[c] A.-J. Kallio, Prof. Dr. S. Huotari
Department of Physics
University of Helsinki, Helsinki
P. O. Box 64, FI-00014, Finland
E-mail: simo.huotari@helsinki.fi

materials under reaction conditions, while operando means the characterization under realistic working conditions with simultaneous online product analysis to guarantee that the system under study is indeed properly working.[46–50] As foreseen in our latest publication on introducing, to the best of our knowledge, the first operando laboratory-based XANES study of multi-element solid catalysts,[29] we enter a new era of advanced catalyst characterization, which comes along with the need for guidelines on how to succeed with this new analytical technique, especially for newcomers in the field.

Performing proper XAS experiments at a synchrotron facility usually involves detailed planning of the experiments and discussions with a responsible beamline scientist not only in the preparation for the beamtime, but also during the experiments. This successful team-science approach is likewise desirable for laboratory-based XAS experiments. Hence, it is important to have a strong collaborative network, which allows to have similar scientific discussions also in the laboratory-based XAS community. If interested scientists can reach out to such a network to discuss the research question, the selection of potential samples, the instrumental approach, and the data analysis, it can be ensured that the requirements for the proposed experiment can be fulfilled at a laboratory-based XAS instrument - or discussed which adaptions need to be done. Such collaborative networks have recently started to develop, not the least due to the first international workshop on laboratory-based spectroscopies, which was held in 2022 in Helsinki (https://www.helsinki.fi/en/infrastructures/center-for-x-ray-spectroscopy/education/workshops-and-schools/international-workshop-on-laboratory-based-spectroscopies-2022), followed by a second workshop in 2023 in Berlin (https://www.tu.berlin/axp/2ter-internationaler-workshop-zu-labor-basierter-spektroskopie).

Besides various self-built setups all over the world,[20,22,23,25–29,51–53] commercial setups are also available from the companies easyXAFS (https://www.easyxafs.com), HP Spectroscopy (https://www.hp-spectroscopy.com), and Sigray (https://sigray.com). Once a newcomer in the field is interested in performing laboratory-based XAS experiments, we recommend to first start a collaboration with more experienced groups and in case there is a stronger interest beyond these first experiments, it might be worth thinking about building or buying an own setup. Especially for ex situ measurements, some research groups offer their setups as service facilities,

Dr. Nina S. Genz studied Chemistry at Technical University Berlin (Germany) and obtained her PhD from the same university (with Prof. Thorsten Ressler). During her postdoctoral stay at Utrecht University, the Netherlands, with a Walter Benjamin Fellowship from the German Research Foundation (DFG), her research focussed on advanced operando characterization of multi-metal CO_2 hydrogenation catalyst materials with a special emphasis on both laboratory-based and synchrotron-based X-ray techniques. Recently, she started a tenure track position at the SuperXAS beamline at the Paul Scherrer Institute (Switzerland) in the field of operando spectroscopy of functional materials.

Mr. Antti-Jussi Kallio started his PhD studies in physics at the University of Helsinki in 2020. Already earlier in his MSc thesis he started working with laboratory-scale XAS instruments. In the PhD studies he has further developed the technique and designed setups that enable operando and in situ XAS studies on thin films, batteries, electrocatalytic fuel cells, photocatalysis, and heterogeneous catalysis.

Dr. Florian Meirer obtained his ScD degree (2008) in technical physics from the TU Wien, Austria (Vienna University of Technology, Prof. Christina Streli). After postdoctoral stays at the Stanford Synchrotron Radiation Lightsource, USA (Schrödinger fellowship, with Prof. Piero Pianetta) and the Fondazione Bruno Kessler, Italy (Marie-Curie co-fund fellowship), he moved to Utrecht University, the Netherlands, to work on spectroscopic and spectro-microscopic methods for the characterization of solid catalysts and related nanomaterials. He is currently Associate Professor and his fields of research include spectro-microscopy, data mining, and chemometrics in the fields of heterogenous catalysis and environmental analysis.

Prof. Dr. Simo Huotari obtained his PhD from the University of Helsinki in 2003. For 7 years after, he was employed at the European Synchrotron Radiation Facility, Grenoble, France, as a post-doctoral fellow and a beamline scientist. Currently, he is the Head of the Department of Physics of the University of Helsinki. He focuses his research in novel analytical tools for materials research offered by X-rays and synchrotron radiation.

Prof. Bert M. Weckhuysen obtained his PhD degree from KU Leuven, Belgium (with Prof. Robert Schoonheydt) in 1995. After postdoctoral stays at Lehigh University, USA (with Prof. Israel Wachs) and Texas A&M University, USA (with Prof. Jack Lunsford), he became a full Professor at Utrecht University, the Netherlands in 2000. His research focuses on the development and use of in situ and operando spectroscopy for studying solid catalysts under both realistic reaction conditions and at different length scales. The aim is to understand reaction and deactivation mechanisms in catalysts that convert feedstock molecules, for various resources, into fuels, chemicals and materials.

which enables a comparatively easy access for interested users. Such facilities are for example the Center for X-ray Spectroscopy at University of Helsinki (https://www.helsinki.fi/en/infrastructures/center-for-x-ray-spectroscopy), and the Clean Energy Institute X-ray Absorption Near-Edge Structure (CEI-XANES) facility located in the Molecular Analysis Facility (MAF) at the University of Washington[20] (https:// www.moles.washington.edu/facilities/molecular-analysis-facility). The benefit of offering the instrumentation as service facility to users is that it is often the new collaborations that drive the continuous development of laboratory-based XAS instruments. The broader the user community, the broader the applications of such novel analytical instruments, and the greater the development of the currently existing setups to spur more advanced experiments to learn more about the properties of functional materials under relevant conditions. Based on this development, laboratory-based XAS becomes increasingly more interesting for a broader community, ranging from catalysis, to geology, biology, energy materials, archaeology, physics, materials science, cultural heritage, and other fields.[6,21,24]

This review article provides a practical view on the use of laboratory-based XAS focused on operando catalysis experiments in transmission mode. We omit the discussion of recent developments of laboratory-based XAS *per se*, as this can be read in the latest review articles from Zimmermann et al.[21] and Malzer et al.[24] It is also not our intention to give detailed insights into the technical parts of laboratory-based XAS setups or to evaluate the different setups. Instead, considering the broad field of possible applications of laboratory-based XAS and the new possibilities for operando characterization, we aim to provide with this review article certain relevant guidelines for those who are entering the field and would like to employ this powerful characterization technique in their research. In what follows, we describe ten steps towards a successful operando laboratory-based XAS experiment. We have decided to focus on an operando laboratory-based XAS experiment in the field of thermo-catalysis as this allows to build on the first operando laboratory-based XANES experiments at multi-metal CO_2 hydrogenation catalysts.[29] However, we would like to emphasize that these guidelines are likewise equally valid for other possible application fields when considering specific requirements, such as an operando cell design.

Ten Steps towards an Operando Laboratory-based XAS Experiment

In an ideal XAS experiment, both XANES and EXAFS should be acquired to obtain a complete data set, but typically due to time limitations, laboratory-based XAS has focused more on the XANES region up to now, because it is faster to be measured. Interestingly, in the last years, machine learning tools were successfully applied to determine the 3-dimensional geometry around the metal species solely based on the experimental XANES without the need of the EXAFS.[54–57] This advancement is especially promising in view of improving and widening the applicability of laboratory-based XAS.

In the following, we will give guidelines on how to prepare for and perform successful operando laboratory-based XAS experiments by discussing ten important steps towards this goal. We aim to make laboratory-based XAS more easily applicable also for newcomers in the field and to help the start of future collaborations allowing for a broader accessibility. In our examples we will focus on XANES experiments, but the discussion is equally valid for EXAFS studies.

1. Determination of the research question, including its suitability for performing laboratory-based XAS experiments

The first step is to determine the research question(s) and to assess whether laboratory-based XAS is suitable to address it. For this purpose, it is important to clearly define the required information, that needs to be extracted to solve the research question. Only if this information can be obtained from laboratory-based XAS, it is reasonable to aim for this technique.

Importantly, just as at a synchrotron facility, safety considerations are paramount for experiments at a laboratory-based spectrometer. Discussing various safety precautions is outside the scope of this article, but we would like to emphasize that such discussions need to be considered when evaluating the suitability for laboratory-based XAS experiments.

Another important decision concerning the suitability of laboratory-based XAS experiments is the required time resolution from the experiments. Compared to similar studies at a synchrotron facility, the time resolution of a laboratory-based setup is significantly lower, making fast processes impossible to follow with the current technology. Depending on the beamline, time resolutions between seconds and milliseconds are easily achievable at a synchrotron facility,[58–61] while one XANES scan takes several minutes or even hours in a typical laboratory-based setup. To give an impression of the possible time resolutions in a laboratory-based setup, we have summarized some selected examples. Bajnóczi et al.,[32] using a water-cooled X-ray tube with a Cu anode at 9 kV and 40 mA, performed XANES of Ni-containing solutions in a custom-built liquid cell and the time for collecting ex situ XANES in transmission mode in a satisfying data quality of the 0.25 M $NiCl_2$ and 0.30 M EDTA solutions with varying KCN concentration was 1 h per sample. Kallio et al.,[62] utilizing a water-cooled X-ray tube with an Ag anode, operating normally at 20 kV and 40 mA, investigated thin CuI and CuO films (12–248 nm) grown on silicon substrates by atomic layer deposition by ex situ and in situ XAS in fluorescence mode. Ex situ XANES of the CuI films was conducted with a counting time of 100 s per step, and each scan was performed twice, which resulted in a total measurement time of 100 min per sample. For CuO films, the ex situ XANES could be collected with a counting time of 2 s per step, resulting in a total scan time of 5 min per sample. Moreover, they performed in situ XANES studies of a 248 nm CuI film to investigate the annealing process at 240 °C in air. Here, the total scan time was 6 min 40 s. In our latest operando laboratory-

based XANES studies, using the above mentioned X-ray tube and settings, we have investigated SiO_2-supported multi-metal catalysts consisting of Ni, Fe, and Cu with a constant total metal loading of 6 wt%.[29] One XANES scan at the Fe or Cu K-edge took 15 min and we averaged two of them, yielding a total measurement time of 30 min at the Fe and Cu K-edge. Conversely, one XANES scan at the Ni K-edge took ~30 min and by averaging 4 scans, the total measurement time resulted in 2 h. The reason for the longer measurement times in the case of Ni K-edge was the coinciding W $L\alpha_{1,2}$ fluorescence lines (at 8335 and 8398 eV) that originated from W contamination on the Ag anode, if the accelerating voltage was set above the W L_3-edge (10.2 keV). Thus, in the case of Ni K-edge, the voltage had to be kept at 10 keV and the current consequently at 2 mA according to the specifications of the manufacturer, reducing the power to 20 W. Importantly, depending on the functional material and the concentration of the element under study, the measurement times in a laboratory-based XAS setup can vary significantly. Being aware of the lower time resolution of laboratory-based compared to synchrotron-based studies, it can be worth to modify the experiment in a way to enable detailed insights by slowing down the processes or planning intermediate steps.

Moreover, the absorption edges of the functional material of interest must be suitable for the laboratory-based setup. Such setups are usually well-suited for transition metals and lanthanides. Published work covers different energy ranges[25,26] enabling the study of K-edges of the 3d transition metals as well as L-edges of 5d transition metals and actinides. It is important to note that soft (up to ~1 keV), tender (roughly 1–3 keV), and hard (>3 keV) X-ray regions typically need different instrumentation and different properties from the samples and their environment. Hard X-rays edges are usually most readily suited for operando experiments to begin with when using laboratory-based XAS owing to their ability to probe samples in complex environments.

2. Choice of the most suitable monochromator crystal, measurement mode, and detector

The next important step is the selection of suitable monochromator crystals. For monochromatizing and focusing of the polychromatic X-ray beam emitted by the X-ray source, crystal analyzers constitute important components of a laboratory-based XAS setup. The crystal spectrometer employs Bragg's law to select a suitable monochromatic X-ray beam energy from the Bremsstrahlung spectrum of a X-ray source. Namely, unlike in a regular X-ray diffractometer, for XAS, it is highly desirable not to have any characteristic X-ray lines in the vicinity of the energy range of investigation, and instead to use the featureless Bremsstrahlung. This greatly helps in obtaining smooth and artefact-free XAS spectra. The monochromator crystal is usually selected to have a Bragg angle as close to 90° as possible, since the effect of geometric aberrations in the energy resolution of the wavelength dispersive spectrometer are then minimized.

The various available laboratory-based XAS setups are usually based on wavelength dispersive crystal spectrometers and can be roughly divided into two general design principles, the non-scanning- and the scanning-type spectrometers.[21,27,63] Depending on the instrument, either spherically bent crystal analyzers (SBCA's) or cylindrically bent crystal analyzers (CBCA's) are used.[21,25,27] SBCA's are frequently employed in Johann/Johannsson geometry setups, while CBCA's are often used in the von Hamos geometry setups. We will focus in the following on SBCA's in a scanning-type Johann geometry (Figure 1d).

Without going too deep into the theory of crystal orientation and manufacturing, it is important to know that different crystal materials and orientations have to be employed for different absorption edges.[64] For further information on the manufacturing of SBCA's, we can recommend for example the paper from Rovezzi et al.[65] addressing the processes in the Crystal Analyzer Laboratory (CAL) at the European Synchrotron Radiation Facility (ESRF), or the websites from NJ-XRS Tech (https://xrstech.com) or Saint-Gobain (https://www.crystals.saint-gobain.com/x-ray-analyzers). For choosing the suitable SBCA for the specific absorption edge of interest, the website from Argonne National Laboratory[66] (https://www.aps.anl.gov/Analyzer-Atlas/Analyzer-Atlas) can be helpful, as based on the entered absorption edge, a table of suitable crystal analyzers will be proposed. When choosing the Fe K-edge, for example, Ge(620) and Si(531) are suitable SBCA's, whereby Ge(620) has a higher energy resolution than Si(531) because of its higher Bragg angle for this photon energy. Roughly speaking, it would be advisable to find a crystal with a Bragg angle between 70–85° for the desired absorption edge. Finally, it is important to be aware that the commonly used Ge analyzers may pose difficulties when working near the Ge K_α and K_β fluorescence lines, which will be excited if the X-ray source acceleration voltage is above the Ge K-edge (11.1 keV).

Moreover, the choice of the most suitable measurement mode, which should be based on the material of interest, is essential in step two towards a successful operando laboratory-based XAS experiment and holds likewise for synchrotron-based experiments. For highly diluted samples with only very low metal (oxide, carbide, or sulfide) concentration and resulting low absorbance steps or thin-films, measurements in fluorescence mode should be preferred to those in transmission mode. Conversely, for functional materials with sufficient absorbance, measurements in transmission mode are generally envisaged as those do not induce self-absorption effects if the sample preparation is done according to steps 6 and 7.[67,68]

Besides the decision on the most suitable measurement mode, that on the detector is essential and dependent on the research question and the availability. Depending on the intended applicability and the spectrometer (scanning- or non-scanning-type[21]), different detectors are reported to be employed in the various laboratory-based XAS setups, for example, the position sensitive Advacam Minipix[62] (https://advacam.com/minipix) based on the Timepix3 chip[69] or Modupix,[26,29] Dectris Mythen[23,32] or Eiger2 R 500 K[28] (https://www.dectris.com), as well as the energy-sensitive solid-state silicon drift detectors (SDD) from Amptek Inc. (https://www.

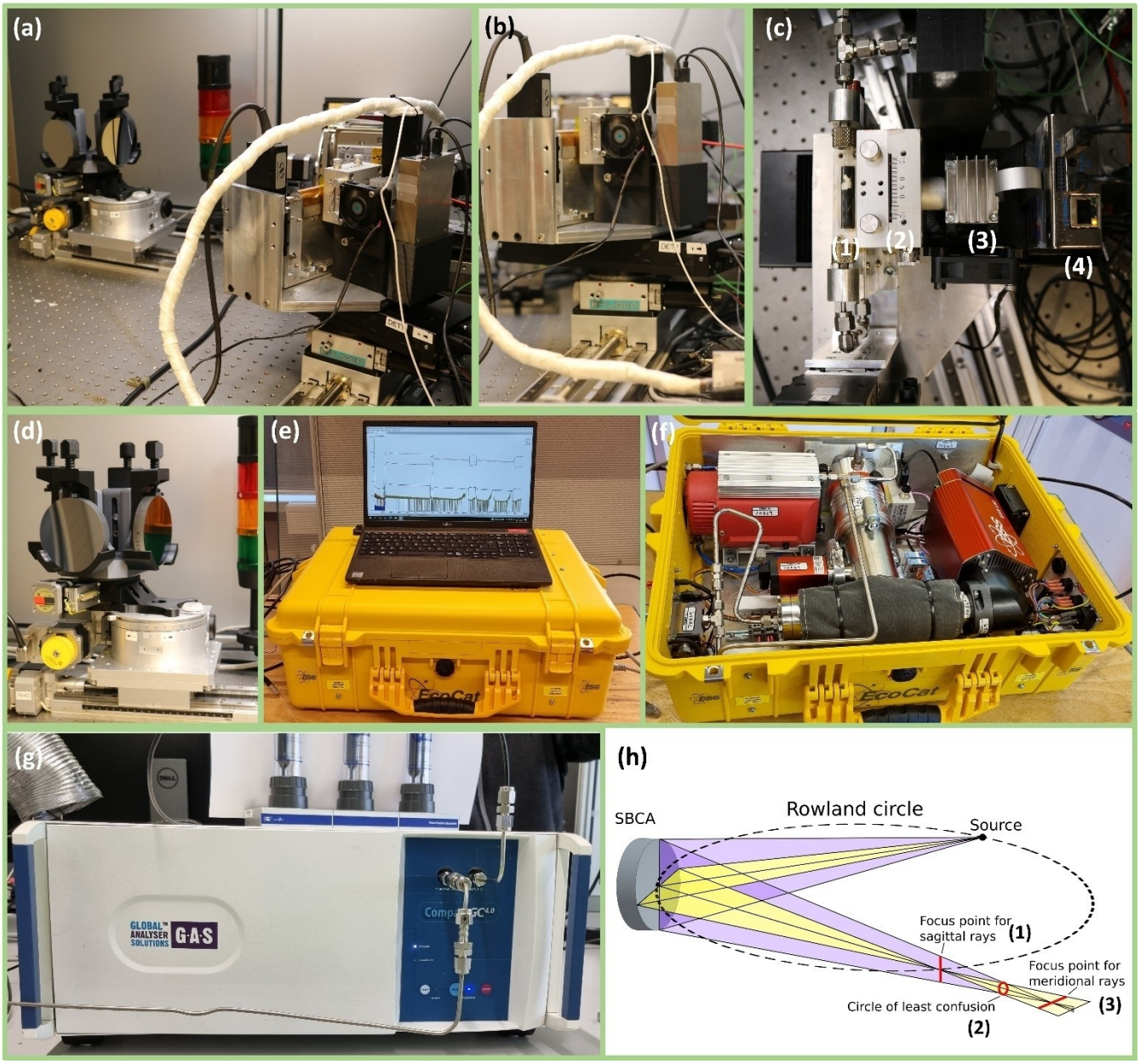

Figure 1. Operando laboratory-based X-ray absorption spectroscopy (XAS) setup (a) with a self-designed sample cell stage (b) where the operando cell is positioned in front of a slit and the detector. Cooling of the detector during heating of the operando cell (c, 1) is ensured by a fan (c, 3) which is inserted between slit (c, 2) and silicon drift detector (c, 4). Photograph of spherically bent crystal analyzers being located in a self-designed crystal exchanger for operando laboratory-based XAS experiments at various absorption edges (d). Photograph of a portable mass spectrometer (MS) (e, f) and a gas chromatograph (GC) (g) being typically used for simultaneous online reactant and reaction products analysis during an operando experiment, both useful for laboratory-based and synchrotron-based XAS experiments. Scheme of three possible X-ray beam geometries (h, 1–3) depending on the focus point and sample geometry, which correlates with the photon efficiency on the sample.

amptek.com) in different modifications,[23,25–27,29] but also SDD detectors from Ketek GmbH (e.g., Vitus H150, https://www.ketek.net) or Hitachi High-Tech (https://www.hitachi-hightech.com). In general, it can be advantageous to use the setup in a flexible mode allowing to change between different detectors. For example, for operando measurements where the catalyst material is located inside a capillary reactor, it can be beneficial to use an imaging detector for the alignment of the capillary and the optimization of the beam size and geometry.[29] Moreover, the possibility to use both a transmission and a fluorescence detector simultaneously constitutes a smart approach for functional materials consisting of different elements of interest. For example, when investigating multi-element materials where some elements are present in low concentrations so that fluorescence mode becomes necessary, while other elements are present in sufficient concentrations which allow for transmission mode, it is convenient to have both detectors installed so that the edge change comes along with the use of the other detector.

After the choice of the most suitable measurement mode and the detector, it is important to consider an appropriate cooling of the detector during the operando experiments when reaching high temperatures. As depicted in Figure 1a–c, in our example setup, the SDD detector is located directly after the slit, which in turn is positioned behind the operando cell. While measuring at elevated temperatures, in our latest study up to 520 °C,[29] the heating of the operando cell radiates also towards the detector. To ensure a safe operation also at high temperatures, we designed an air-cooling for the detector by a laterally installed fan (Figure 1a–c).

When planning an operando experiment, it is always advisable to carefully choose the most suitable detector, from those that are available to the instrument at the time of study, since a proper choice of the detector has direct consequence on the ease of alignment, data processing and eventually on the data quality.

3. Choice of appropriate product analysis technique

The third step towards the design of a successful operando laboratory-based XAS experiment concerns the choice of the appropriate product analysis technique. Depending on the functional material and the field of application, different analysis techniques might be suitable. For gas-phase reactions, online gas chromatography (GC) and mass spectrometry (MS) are commonly employed (Figure 1). While GC allows for the direct quantification of the reactants and reaction products, the choice and availability of suitable columns as well as related time resolution are crucial parameters for the success of an operando experiment where time-resolved catalytic performance is correlated with time-resolved spectroscopic data.[70,71] Although online MS does not directly allow to quantify the reactant and reaction products, a calibration is in principle possible. MS is particularly advantageous for following fast processes (e.g., $<$ min), which does not yet hold for laboratory-based XAS spectroscopy experiments. However, the product detection via MS is based on the detection of charged fragments of the initial products, which allows to follow the formation and evolution of various products simultaneously. Briefly speaking, the reaction products are introduced into the MS where in a first step their ionization takes place. Importantly, the ions can either be fragments, clusters, or single atoms. Subsequently, these charged fragments or ions are separated by their mass-to-charge (m/z) ratio, which in turn allows for an analysis of the inserted reaction products.[72,73] Conversely, online GC is based on the different interactions between various reactants and reaction products and the column, yielding a sequential product detection whereby the differentiation of overlapping products becomes challenging. The very basic principle of a GC can be explained as follows: the reaction products, being the analytes, are injected into the gas chromatograph and a carrier gas, the mobile phase, transports the analyte through the column. The column contains the so-called stationary phase, which interacts with the various analytes during the transport through the column. Based on these interactions, being also described as phase transfer reactions, the various analytes are retained differently, which in turn results in different times when the analytes exit the column towards the detector. Based on this separation process, the reaction products can be analyzed.[70,71] Depending on the research question, one should decide which product analysis is the most suitable in view of expected reaction products and availability for the planned operando laboratory-based XAS experiments.

4. Search for suitable reference materials

Carefully chosen and suitable reference materials are key for a successful analysis and interpretation of the recorded XAS data, which holds for both laboratory- and synchrotron-based experiments. Whenever planning a XAS experiment, considerations of suitable reference materials should be a crucial step. Reference materials should have well-known chemical compositions and electronic properties, being similar to those of the actual functional materials. For example, a linear combination fitting (LCF)[1,74] of the XANES spectra to references makes only sense if the chosen set of reference materials is relevant and complete enough. Even if the chemical composition and electronic properties of the functional materials are not yet known, or only very little information is available, it is important to consider various reference materials, which might represent the functional materials. For this purpose, compounds of bulk materials are often used. However, for functional materials, for example, supported metal (oxide, carbide, or sulfide) nanoparticles, bulk reference materials might not be well suited for a structural comparison.[75–77] Hence, it is worth considering "homemade" reference materials, for example, self-synthesized materials with the same or at least a similar nanoparticle size as that of the actual functional material. However, a detailed characterization of these materials should be conducted before using them as references. As a very basic approach for the selection of reference materials, we recommend considering all possible compounds which can in theory be formed with the functional material of interest under the specific reaction conditions. For example, if the functional material contains iron oxidic species and the planned experiment involves a treatment under reducing conditions, a good starting point is a set of the various possible iron oxides, that is, iron oxides where iron has different oxidation states, and the pure metal (Fe). Moreover, depending on the material, one might additionally consider various iron carbides, iron (sub−) oxides and/or iron hydroxides. If the functional material contains not only iron oxides but additional elements, it is also important to consider possible mixed compounds. This brief example already demonstrates that it is essential to consider all possible reference materials of importance, which can de facto easily become a broad variety. However, the better the choice of the reference materials, the easier the data analysis after the experiment.

5. Spectrometer preparation and alignment

The fifth step towards a successful operando laboratory-based XAS experiment is the spectrometer preparation and alignment. After choosing the suitable monochromator crystal for the absorption edge of interest (see step 2), it is important to precisely align the crystal. Despite a precise manufacturing, crystal analyzers may possess a miscut, which has to be accounted for during the alignment.[78] As the alignment of the crystal is not trivial, but needs expert skills, we advise the user to ask for help from collaborators or vendors who provide the laboratory-based XAS setups. This is important as the alignment process must be repeated for each crystal and the planned experiment will significantly gain in quality by properly aligned crystals. Briefly speaking, first, a rough optical alignment with a laser pointer can be conducted. To this purpose, the laser pointer should be positioned at the X-ray source and point towards the crystal. Once the rough alignment with the laser pointer is finished, the precise alignment with X-rays can start. For more details, we refer the interested user to the robust alignment procedure published by Mortensen and Seidler.[78] We would like to mention that a position sensitive detector is particularly helpful for the precise alignment as it allows to actually visualize the beam shape.

Besides the alignment, the spectrometer preparation also includes the design of possibly required customized parts, such as cell stages for the various sample environments, or holders for the detectors. While designing and operating our operando laboratory-based XANES setup, we designed most of the essential parts ourselves and fabricated most of them via 3D-printing. This approach was especially valuable in terms of time-saving reparations or modifications of the setup, but also cost-effective. After designing the 3D-model, the printing can take between a few minutes up to several hours/days depending on the model and can be scheduled in a smart way, for example, overnight or during the weekend. Whenever possible, we encourage the users to try this approach as self-made parts can precisely be designed for the specific setup and purpose, which is more difficult if not impossible for commercially available parts.

Optimization of the X-ray beam geometry constitutes another important step of the spectrometer preparation. The geometry of the X-ray beam crucially affects the photon efficiency on the sample, and hence, the quality of the resulting XAS spectra. Therefore, it is important to optimize the X-ray beam geometry to the sample geometry with the goal to enable the highest photon efficiency on the sample, that is, to generate the largest overlapping area of X-ray beam and sample.

In principle, the beam size can be adjusted by the user when using slits. For a laboratory-based XAS setup, the Rowland circle geometry in combination with a point X-ray source and SBCA's at Bragg angles different to 90°, the so-called astigmatism error of the SBCA's becomes relevant. The astigmatism of the SBCA's is similar to that of an optical lens and generates two separated line images, which are perpendicular to each other.[29,79] This in turn results in three different X-ray beam geometries. There are two line foci, perpendicular and parallel to the Rowland circle, which are located on the Rowland circle and outside of it, respectively. In the middle of these line foci, a round blur spot is formed (Figure 1h). Depending on the size and the shape of the sample and the detector, the optimal use of the focal points can be planned for maximising the efficiency of the operando experiment.

The line focus that is located at the nominal position on the Rowland circle is here referred to as the vertical X-ray beam geometry (Figure 1h, 1), since most often in laboratory-based XAS the Rowland circle is horizontal – a simple consequence of the fact that the optical elements are typically assembled on an optical table. Accordingly, this vertical X-ray beam geometry is most commonly employed for laboratory-based XAS experiments. However, if the sample has a round shape and needs to be located in front of the detector, one could consider optimizing the alignment so that the sample is located on the blur spot (circle of least confusion, Figure 1h, 2). In case the sample is a wafer, which is usually the case for ex situ reference measurements (see step 6), it can be optimal to place it directly in front of the X-ray source, that is, in the white beam, in which case the beam footprint on the sample remains unchanged regardless of Bragg angle. When doing so, it is important to be aware of the possible background noise due to fluorescence radiation from the sample. However, for radiation sensitive samples, for example, electrolyte solutions, it can be advantageous to place the sample on the detector side rather than in front of the X-ray source, and hereby, reduce the influence of a possible beam damage. On the other hand, if the sample is located inside a linear capillary reactor, as recently described for multi-metal CO_2 hydrogenation catalysts,[29] a horizontal line-focus of the X-ray beam (Figure 1h, 3) can be the optimal geometry as the photon efficiency on the sample can be maximized by adjusting the size of the horizontal line-focus so

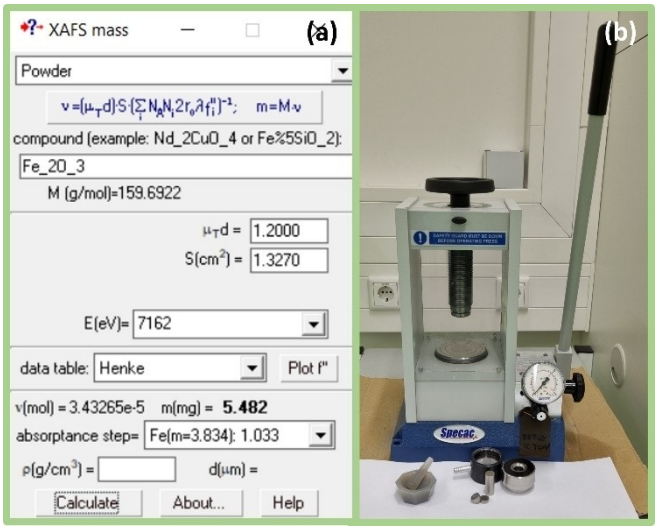

Figure 2. XAFSmass software[82] (a) for calculating the required amount of reference material (Fe_2O_3) for a specific total absorption and given sample area for a powder sample together with the resulting edge jump (absorptance step) as well as the pressing tools (b), i.e., mortar, dies, press for pressing the corresponding self-supporting wafer.

that it matches the dimension of the catalyst bed inside the capillary. This horizontal line-focus can be achieved by positioning the sample and detector outside the Rowland circle at the position of the sharpest line-focus of the X-ray beam (focus point for meridional rays).

The distance of the envisaged focal spot is crucial, and the focal spot size depends on the Bragg angle. In general, the smaller the Bragg angle, the larger the focal spot size, regardless of whether a line foci or a round blur spot is used. Hence, we advise the user to first determine the distance of the optimal focal spot and the monochromator crystal(s) of interest, and subsequently save the correct positions of the detector or the sample in the measurement macro so that those can automatically be set during the operando run.[29] Practically, this determination, for example, the optimal horizontal line-focus can be performed by starting at the position of the vertical line-focus, hence, with the sample and detector being positioned on the Rowland circle and moving further outside while comparing the resulting X-ray geometry. Importantly, this procedure can equally be used for determining the optimal round X-ray geometry.

6. Ex situ reference measurements

After selecting suitable reference materials, ex situ reference measurements should be performed and before starting those, it is necessary to calculate the optimal amount of the reference material for the transmission experiment. For this purpose, different programs are available, for example, XAS Powder Sample Weight Calculator from Stanford Synchrotron Radiation Lightsource[80] (https://www-ssrl.slac.stanford.edu/smbin/mucal-webnew.pl), XAFS Transmission-Mode Sample Analysis from the IXAS[3] portal (https://xraydb.xrayabsorption.org/transmission_sample), Hephaestus software,[81] or XAFSmass.[82] The calculation is equally valid for laboratory-based and synchrotron-based XAS experiments and based on the absorbance of the reference material, the dimension of the self-supporting wafer (for powder measurements), and the absorption edge of interest. When using, for example, the open access program XAFSmass,[82] specific information besides the chemical composition such as, for a powder sample, the sample area, together with the total absorption and the chosen absorption edge need to be filled. Based on this information, the program yields an expected absorptance step (edge jump) together with the required amount of sample. Allowing a total absorption between 1.2 and 2.0 is generally a good starting point. Importantly, the resulting edge jumps should ideally be around 1.0 for good data quality. For resulting edge jumps of 1.5 and higher, the mass of the reference material should be reduced to avoid possible thickness effects.[83] For illustrative purposes, we chose Fe_2O_3 as reference material (Figure 2a). With an area of 1.327 cm^2, resulting for a wafer diameter of 13 mm, and a total absorption of 1.2, 5.482 mg of the powder will result in an edge jump of about 1.0 at the Fe K-edge. Hence, we would need about 5.5 mg of Fe_2O_3 for pressing a suitable reference wafer. Considering the size of the dies (13 mm diameter) and the small amount of required Fe_2O_3 powder it becomes evident that we cannot press a wafer consisting only of the reference material, but we will need a diluent. In general, boron nitride (BN), cellulose, polyethylene (PE), or starch constitute suitable diluent materials. Moreover, commercially available X-ray fluorescence (XRF) binding materials, such as ultrapure boric-acid-based materials, can likewise be employed as diluent material. As rule of thumb, a "good wafer" consists of about 100 mg powder, including both reference and diluent material. Hence, following our example, we mix 5.5 mg Fe_2O_3 with any (almost) X-ray transparent diluent, for example, starch, in a mortar, and afterwards use 13 mm dies in the pressing tool to create a self-supporting wafer (Figure 2b). Depending on the reference material and diluent, it is in general sufficient to apply 0.5-2 t for 3–10 s for pressing stable self-supporting wafers. Importantly, the preparation of homogeneous samples is crucial for the measurements. Hence, it is essential to ensure a proper mixing of the reference material with the diluent, but also to avoid a too coarse particle size. Otherwise, for inhomogeneous samples, so-called pinhole effects can occur where a part of the incident X-rays is transmitted without interacting with the absorbing element.[83]

We would like to mention here that depending on the number of reference materials, pressing wafers can easily become a time-consuming task. Hence, we advise to consider this in the preparations for the experiment. Moreover, we have experienced that reference wafers with BN as diluent are often fragile and once pressed, the wafer is very adhesive to the dies, resulting in a high failure rate. Hence, it can be advantageous to use cellulose, starch, or PE to facilitate the pressing procedure.

After preparing the reference wafers, it is important to decide on the most suitable approach to mount those onto a holder, in our example an ex situ sample wheel. Depending on the stability of the self-supporting wafers, it can be advantageous to wrap the wafers between Kapton tape. Another benefit of wrapping the self-supporting reference wafers into Kapton tape is the possibility to easily tape and remove those from the ex situ sample wheel (Figure 3a) so that those can be reused for various reference measurements. Besides, the direct use of self-supporting reference wafers without a tape is also possible. Hereby, it is important to handle the wafers with care when mounting, that is, taping, those onto the ex situ sample wheel. A third possibility to mount reference materials onto the ex situ sample wheel is the use of washers instead of self-supporting wafers. When doing so, all steps described above are equally valid, but instead of using the dies and the pressing tool to press self-supporting wafers, the mixture of reference material and diluent is directly filled into the washer, which is positioned onto a tape (either Scotch tape or Kapton tape) to keep the powder in place. After compressing the loose powder inside the washer with a pestle, the top of the washer is also taped, in order to fix the compressed powder. Subsequently, the washer can be mounted onto the ex situ sample wheel. These approaches to mount reference materials onto the ex situ sample wheel for reference measurements are, however, only applicable for chemically stable reference materials.

For air-sensitive reference materials, the mixture of the reference material and diluent should be produced in an inert atmosphere, hence, in a glovebox, sealed in an airtight sample holder, and brought to the experiment station under the inert gas atmosphere. For this purpose, we have designed an airtight wheel-shaped sample holder, which can be filled with several samples inside a glovebox. Accordingly, each sample in the inert atmosphere can be placed between two Kapton foils, being sealed by an O-ring (e.g., Viton), and mounted between two metal slides of the airtight wheel (Figure 3b). The screws around each sample position allow for a sealing and exclusion of air-contact also after taking the airtight wheel out of the glovebox (Figure 3c).

Additionally, measurements of the pure metals, which are usually purchased as thin foils with a thickness optimized to be of the order of the absorption length are essential. The energy calibration is generally based on the reference metal foil spectra (see for example, http://exafsmaterials.com/Ref_Spectra_0.4MB.pdf). To this purpose, the metal foils can, similar to the chemically stable reference wafers, be taped onto the ex situ wheel and after positioning the ex situ wheel in front of the X-ray source at a motorized holder, automated reference measurements can be performed.[29]

Figure 3d-f depicts several ex situ XANES from reference materials measured with the ex situ as well as airtight wheel together with metal foil measurements. Comparing the different XANES, it is evident that neither the use of the airtight wheel nor the preparation as self-supporting wafers, wafers being wrapped in Kapton tape, or washers, induce a significant effect on the data quality. Hence, the decision on the most suitable reference material preparation is up to each user as long as a suitable edge jump and homogeneous reference preparation is considered.

Although various XAS databases exist, where spectra of common reference materials are collected, we advise to avoid using such reference spectra as those are usually measured at a synchrotron facility. Differences in, for example, energy resolution and S/N ratio and generally different measurement conditions between different data sources, especially between a synchrotron facility and a laboratory-based spectrometer, may render comparisons difficult. In general, it is always beneficial to measure the reference materials with the same setup which is used for the measurements of the functional material. Nevertheless, we would like to name a few of these databases for the newcomers in the field: https://xaslib.xrayabsorption.org/elem, http://ixs.iit.edu/database, https://www.sshade.eu/db/fame, https://pfxafs.kek.jp/xafsdata/list.php, or https://mdr.nims.go.jp.

7. Operando cell preparation

The next step towards a successful operando laboratory-based XAS experiment constitutes the proper operando cell preparation. It is worth mentioning that the operando cell preparation is not limited to laboratory-based XAS experiments but equally important for similar synchrotron-based experiments. In what follows, we will explain the cell preparation based on our home-build operando cell for thermo-catalytic applications[29,84] and we omit a comprehensive discussion of different operando cell designs. The operando cell itself constitutes an indispensable component for the planned experiments and it is worth evaluating different design principles and their suitability for the specific research question. While doing so, it is highly advisable to consider the design of a cell optimized specifically for laboratory-based XAS. It is in general possible to use cell designs being optimized for synchrotron-based XAS, X-ray scattering, or X-ray diffraction, but those might result in a decreased photon collection efficiency in a laboratory-based XAS spectrometer.

Before starting the operando measurements of the functional material, it is important to determine the absorbance, and if necessary, to choose a suitable diluent for optimizing the transmittance of the functional material. In case the absorbance of the functional material is already suitable, the sample material, in case of a powder, should be sieved to achieve homogeneity. Subsequently, the sieved sample fraction can be loaded into a glass or quartz capillary, in our cell with an inner diameter of 96 mm. Hereby, two quartz wool plugs are used to keep the powder bed in position in the middle of the capillary (Figure 4a, 1). The sufficient compression of the functional material when loading it into the capillary is essential to avoid holes in the powder bed during the operando measurements or moving of the complete bed inside the capillary. The length of the catalyst bed has to be determined based on a compromise between the desired gas hourly space velocity (GHSV) and the optimal heating possibilities being related to the heater geometry. It is always recommended to optimize the amount of functional material to ideally enable the comparability with further characterization techniques. Once the functional material is loaded into the capillary, the capillary can be inserted into the reaction cell. In the here presented operando cell, both ends of the capillary are mounted into rubber ferrules, and subsequently tightened with steel nuts to ensure a gas tightness (Figure 4a, 2). Additionally, a thermocouple is inserted into the capillary, next to the powder bed, to enable the control of the actual bed temperature. Finally, a Kapton cap with two metal shields between the infrared heaters and the capillary is mounted onto the cell to avoid interference with air circulations in the room during the experiment, which would affect the temperature stability of the capillary (Figure 4a, 3). It should be noted that the here described general principles for the operando cell preparation will remain applicable for various operando cells, even if the detailed steps might differ slightly. Generally speaking, the homogeneity of the sample and the comparability with other techniques, i.e., the catalytic conditions in view of for example GHSV and catalyst mass, should be given as well as the proper location of the sample inside the operando cell, and a suitable gas and temperature control during the experiment.

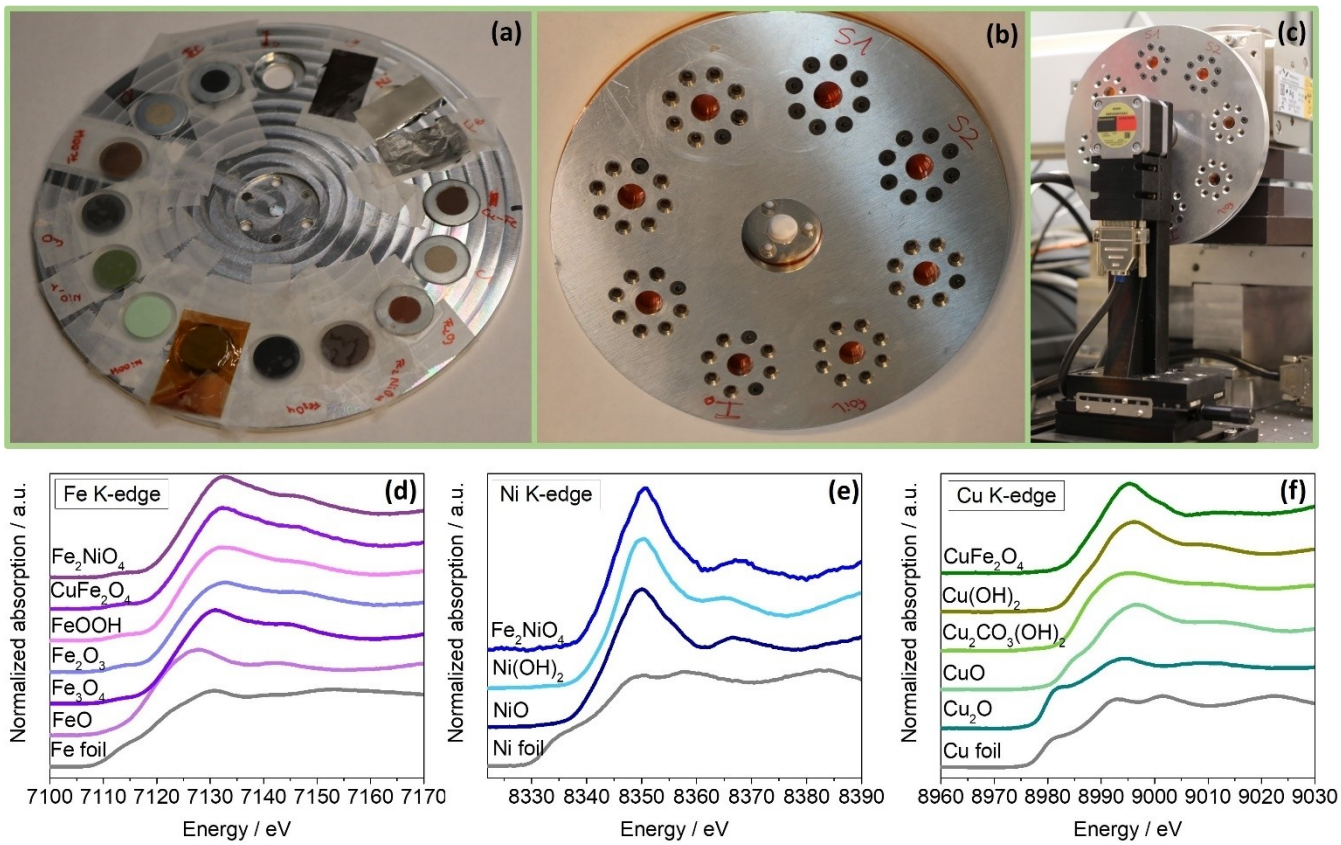

Figure 3. Ex situ sample wheels for chemically stable (a) and air-sensitive (b) reference compounds, being positioned directly in front of the X-ray source at a motorized stage (c) which allows to automatically rotate to the various sample positions on the wheel, together with examples for various ex situ reference measurements in the ex situ wheel for chemically stable references and the airtight wheel at the Fe (d), Ni (e), and Cu (f) K-edges making use of a laboratory-based X-ray absorption spectroscopy (XAS) instrument. The chemically stable reference materials (a) were prepared as self-supporting wafers (being directly taped onto the wheel), wafers being wrapped in Kapton tape (orange-coloured), or washers (silver-coloured rings). All measurements were performed using a polychromatic Ag-tube (source size 0.4 x 0.8 mm^2), a silicon drift detector, and spherically bent crystal analyzers (Si(531), Si(551), Si(553) for the Fe, Ni, and Cu K-edge).

8. Test measurements for time calculations and data quality check

The next step towards a successful operando laboratory-based XANES experiment comprises ex situ test measurements and estimation of the expected data quality. Before starting the operando experiment, it is important to perform ex situ test measurements with the functional material being loaded into the operando cell (Figure 4b). At this stage of the experiment, it is still possible to finetune and change some parameters. Hence, sufficient time should be planned for such test measurements. Ideally, the conditions of these test measurements should be as similar as possible compared to the planned operando conditions. After performing the first ex situ test measurements, it might be worth to consider further measurements at ambient temperature but with a gas flow (for thermo-catalytic experiments). Importantly, the total gas flow should be equal or at least similar to that of the planned operando measurements but with inert gas instead of reaction gas to avoid any structural chances of the functional material during these test measurements. Hereby, it is enabled to control the powder bed location and possible movements when starting the gas flow. Moreover, based on such test measurements, an estimation of the expected data quality becomes possible. Similar to thermo-catalytic operando experiments, the ex situ test conditions for, for example, electro- and photo-catalytic experiments should likewise be as similar as possible compared to the subsequent operando experiments.

In order to control the consistency of the data, one should plan the experiment strategy so that each spectrum should be measured at least twice under the same reaction conditions. This allows to compare them and if they are equal within the statistical accuracy, they can be merged to increase the signal-to-noise (S/N) ratio for the further data analysis. However, if they are not equal, the reason for this systematic uncertainty should be investigated in detail. As the S/N improvement correlates with the square root of the counts, an improvement of a factor of 2 can only be achieved by merging 4 scans. Figure 4c demonstrates exemplarily the S/N improvement of Ni K-edge XANES by merging 4 scans compared to one single scan. Hereby, it is important to balance between a sufficient S/N ratio and a reasonable measurement time of the operando experiments. Importantly, only after deciding on the necessary number of merged spectra, it is possible to calculate the

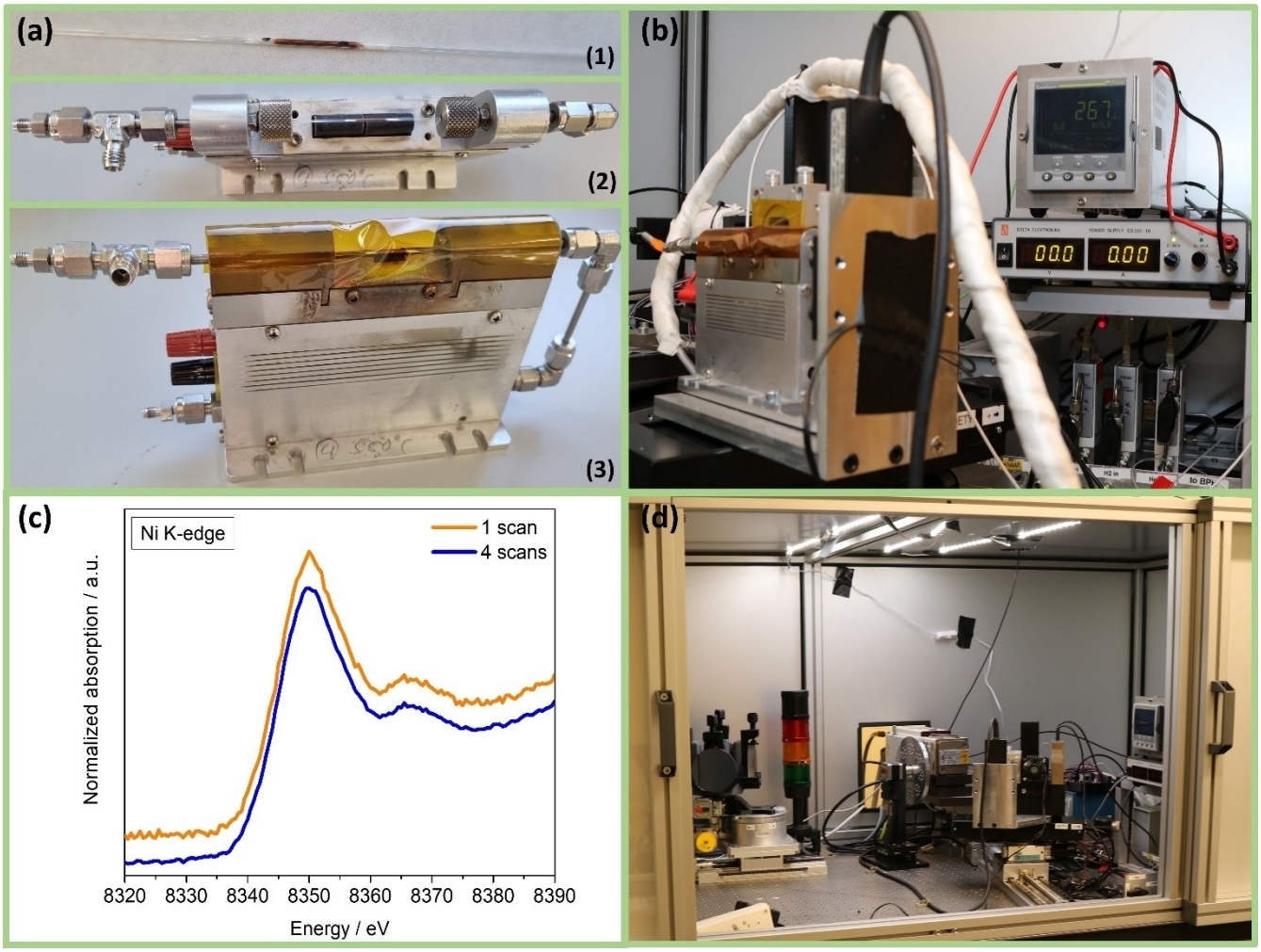

Figure 4. Prepared glass capillary with a 1 cm catalyst bed between two quartz wool plugs (a, 1), being inserted into the reaction cell (a, 2), and the final position of the capillary in the reaction cell with the Kapton cap to exclude temperature fluctuations from air circulations (a, 3). Operando reaction cell with a catalyst powder located inside the capillary and connected to the temperature control and gas dosing system (b) for ex situ test measurements together with the resulted Ni K-edge XANES at room temperature when using one single scan or four scans being merged (c). The XANES were collected for a bimetallic Ni–Fe/SiO_2 catalyst with a Ni loading of 5 wt% at ambient temperature with a gas flow of 10 ml/min Helium. Photograph of an operando laboratory-based XANES setup[29] before starting the experiment to investigate the properties of a solid catalyst at work (d).

measurement time, being indispensable for the adjustment of the "chemical parameters" which will be discussed in step 9.

9. Design of the operando experiment

The design of the operando experiment constitutes the last essential step. Exemplarily, we will continue focusing on a thermo-catalytic experiment as this is our main field of expertise. For further reading on in situ and operando XAS in general, we would like to refer the reader to several review and perspective articles as well as textbooks.[4,6–8,10–12,85]

After deciding on the experimental program, including gas composition, gas flow, temperature program, heating rates, and holding times at the various reaction steps, it is important to combine these "chemical parameters" with the "X-ray parameters", comprising time for one XANES scan and envisaged total time for each reaction step and/or absorption edge, for example, when considering a certain number of merged spectra or measurements at various absorption edges. For the "chemical parameters", it might be envisaged to use a software, amongst others LabVIEW, and create a measurement program which controls both the gas and temperature conditions for the various reaction steps. While for controlling the spectrometer, the software SPEC (https:// www.certif.com/spec.html) or BLISS (https://bliss.gitlab-pages.esrf.fr/bliss/master) can be considered. Moreover, for the "X-ray parameters", a measurement macro should be designed, which allows to start the XANES measurements once and keep those running during the complete LabVIEW program. Especially for temperature-programmed experiments, it is important to adjust the heating rate to the measurement time for the XANES scans. Hence, depending on the necessary time resolution, a lower heating rate might be considered in order to match the scan time. Additionally, it might be worth to adjust the X-ray and LabVIEW times to the product analysis times, that is, when using a gas chromato-

graph one chromatogram takes a specific amount of time and in some cases it might be advantageous to wait with starting the next reaction step until the end of a chromatogram or the beginning of the next. Important for operando XANES at multiple absorption edges is to define an efficient order of the various absorption edges, consider times for crystal exchange and the corresponding parameters, such as, Bragg angles, X-ray tube settings, or position for the sharpest line focus of the X-ray beam when using the design principle of our recently introduced setup.[29] The time for adjusting these settings will add to the total measurement time per scan.

Additionally, another considerable point when designing the operando spectroscopy experiment where gases are involved is the calculation of the expected gas consumption. Depending on the gas infrastructure, this could be a crucial parameter, which should at least be considered. When measuring for several days, it is important to ensure a sufficient volume of gases is available for the complete operando run. A gas bottle exchange during the running experiment is challenging as it can easily interrupt the measurement and should ideally be avoided. Hence, a gas availability should be ensured before starting the operando experiment.

In general, the design of the operando laboratory-based XAS experiment also includes the decision on a priority list and a smart sample order. Starting with the most important and most valuable sample in terms of deducible knowledge for subsequent measurements is advantageous. Let us illustrate this with an example from our first operando laboratory-based XANES studies of multi-metal CO_2 hydrogenation catalyst materials. For this study, we were interested in three monometallic as well as several bi- and trimetallic catalyst materials. As the total metal loading was kept constant, we knew that the monometallic catalysts possess the highest metal loading, hence, we would expect the best S/N ratio of the resulting spectra. Moreover, as the bimetallic catalyst materials are combinations of the elements from our monometallic catalysts, we decided to first focus on the monometallic catalysts. Our intention was to gain first insights into the systems with the highest possible data quality, so that the data analysis should be less challenging compared to the lower loaded samples.

Finally, in view of the comparatively long measurement times of operando laboratory-based XANES experiments, the possibility for a remote access to the X-ray control computer, and ideally also to both the product analysis and gas/temperature control computer, as well as the possibility to install a webcam inside the setup, is highly recommended. In contrast to experiments at a synchrotron facility, 24 h shifts are not mandatory for laboratory-based experiments. However, as interruptions of the measurement macro, leakages of the capillary or operando cell, interruptions of the product analysis, or issues with the various motor movements can always occur, a remote access and the possibility to check the setup via webcam can be very convenient and time-saving. Such a remote access allows for frequent checking of the measurement progress and possible interventions without the need to be 24 h present for operando laboratory-based XANES experiments which last several days.

10. Performance of the operando laboratory-based XANES experiment

After the previous nine steps have been accomplished, the basis for a successful operando laboratory-based XANES experiment is established (Figure 4d). As general remark, we recommend to always ensure the X-ray tube is fully warmed-up before starting any measurements in order to avoid possible I_0 drifts. Importantly, before starting the operando measurement, once everything is prepared for the start, we advise to first perform incident beam, I_0, measurements, which allows to already check the resulted data during the operando run. Once the I_0 measurements are finished, the operando experiment can be started. Depending on the designed experiment, it might be worth to first start the X-rays and to perform some room temperature measurements to ensure the measurement macro is working smoothly. Subsequently, the "chemical parameters", for example, temperature and gas delivery program, as well as the online product analysis can be started. In some cases, it can be necessary to start the different programs simultaneously, which should be decided during step 9, the design of the experiment. Based on our experience, the pre-recorded I_0 measurements are of great importance for the first data analysis during the ongoing measurement to ensure the experiment proceeds as expected, for example, in terms of reduction temperature. Ideally, the X-ray measurement macro should allow for a smooth run of the measurement and the LabVIEW program (holds likewise for other software packages), should enable this for the "chemical parameters". Finally, it is worth mentioning that long-term stability tests of the spectrometer are advisable, especially when performing operando laboratory-based XAS studies of a multitude of catalyst materials, which can easily take several days or weeks. Such tests can be performed by frequent measurements of reference metal foils.

Summary and Outlook

Laboratory-based XAS develops rapidly, and we foresee a bright future of this powerful characterization technique. Especially the possibility to perform operando experiments opened a new era of advanced characterization and constitutes an interesting development for various applications in fields, such as catalysis, fuel cell, and battery research, as well as physics, geology, and environmental science. Flexible setups enable the use of different detectors and measurement modes, and hence, the applicability of operando laboratory-based XAS ranges from bulk materials towards highly-diluted samples or even thin-films.

Operando laboratory-based XAS has been successfully performed in the XANES region up to date in the available literature. However, it is certainly not limited to the XANES region, and the experiments can equally be expanded towards the EXAFS region. The determining reason why EXAFS studies in the laboratory are currently limited to ex situ measurements, is the necessary measurement time. Compared to XANES studies, EXAFS studies require in general an order of magnitude

longer measurement times, making operando laboratory-based EXAFS experiments very challenging.

Concerning the further possibilities of laboratory-based XAS, we believe the field of operando spectroscopy has changed significantly and besides focusing on XAS studies, the combination of various techniques might become available in the near future. If we can perform operando laboratory-based XAS, we can also combine this technique with further characterization tools, such as UV-Vis and Raman spectroscopy, or X-ray diffraction and scattering methods. While the combination of various analytical techniques under operando conditions is frequently applied at synchrotron facilities, those can likewise be performed in a laboratory-based setup. Such a multimodal operando approach will turn laboratory-based XAS into an even more powerful characterization tool, which will foster materials design and further development.

With this review article, we present a series of steps towards a successful operando laboratory-based XAS experiment, which constitute in our view important guidelines for newcomers in the field. These guidelines are intended to help scientists on how to prepare for and perform an operando laboratory-based XAS experiment, irrespectively whether the setup is a commercial or a self-built one. By focusing on the practical rather than the theoretical aspects, we aim to address the broad field of possible applicants. It is important to mention that the proper operando cell design is crucial for the success of the planned experiment, which, however, exceeds the scope of this article. When planning an operando laboratory-based XAS experiment, the availability of a suitable operando cell should be given. Having the presented guidelines in mind, we encourage interested scientists to define their research goal, as described in step number one, and if an own laboratory-based XAS setup is not available, reach out to research groups that have such setups. The enlargement of the international collaborative network in the field will not only speed up the further development of operando laboratory-based XAS, but also help to establish this technique as routine analysis tool in the laboratory.

Acknowledgements

N.S.G. is grateful for funding by the German Research Foundation (DFG, 452243354). A.-J.K. and S.H. acknowledge the Academy of Finland (grant 295696) for funding. A.-J.K. is additionally supported by University of Helsinki Doctoral Programme for Materials Research and Nanoscience and the Jenny and Antti Wihuri foundation (00200134). The Netherlands Research Council (NWO) is acknowledged for the general funding of this research work in the form of a Gravitation Program "Multiscale Catalytic Energy Conversion" (MCEC).

Conflict of Interests

The authors declare no conflict of interest.

Data Availability Statement

The data that support the findings of this study are available from the corresponding author upon reasonable request.

Keywords: X-ray Absorption Spectroscopy · Operando Characterization · Laboratory-based Experimentation · Functional Materials

[1] S. Calvin, *XAFS for Everyone*, Taylor & Francis Group, LLC, Boca Raton, **2013**.
[2] P. Willmott, *An Introduction to Synchrotron Radiation: Techniques and Applications*, John Wiley & Sons, Ltd, Hoboken, **2011**.
[3] "IXAS: The International X-ray Absorption Society," can be found under https://xrayabsorption.org/, (accessed 7 November 2022).
[4] Y. Iwasawa, *J. Catal.* **2003**, *216*, 165–177.
[5] Y. Iwasawa, K. Asakura, M. Tada, *XAFS Techniques for Catalysts, Nanomaterials, and Surfaces*, Springer International Publishing, Cham, **2017**.
[6] J. A. Van Bokhoven, C. Lamberti, *X-Ray Absorption and X-Ray Emission Spectroscopy – Theory and Applications*, John Wiley & Sons, Ltd, Chichester, **2016**.
[7] A. I. Frenkel, J. A. Rodriguez, J. G. Chen, *ACS Catal.* **2012**, *2*, 2269–2280.
[8] S. R. Bare, T. Ressler, *Adv. Catal.* **2009**, *52*, 339–465.
[9] P. Fornasini, R. Grisenti, *J. Synchrotron Radiat.* **2015**, *22*, 1242–1257.
[10] J. Singh, C. Lamberti, J. A. Van Bokhoven, *Chem. Soc. Rev.* **2010**, *39*, 4754–4766.
[11] S. Bordiga, E. Groppo, G. Agostini, J. A. Van Bokhoven, C. Lamberti, *Chem. Rev.* **2013**, *113*, 1736–1850.
[12] J. Timoshenko, B. Roldan Cuenya, *Chem. Rev.* **2021**, *121*, 882–961.
[13] J. Als-Nielsen, D. McMorrow, *Elements of Modern X-Ray Physics*, John Wiley & Sons, Ltd, London, **2011**.
[14] J. Evans, *X-Ray Absorption Spectroscopy for the Chemical and Materials Sciences*, John Wiley & Sons, Ltd, Chichester, **2018**.
[15] G. Bunker, *Introduction to XAFS - A Practical Guide to X-Ray Absorption Fine Structure Spectroscopy*, Cambridge University Press, New York, **2010**.
[16] M. Newville, *Rev. Mineral. Geochemistry* **2014**, *78*, 33–74.
[17] P. Glatzel, U. Bergmann, *Coord. Chem. Rev.* **2005**, *249*, 65–95.
[18] A. I. Frenkel, *Chem. Soc. Rev.* **2012**, *41*, 8163–8178.
[19] "Lightsources.org," can be found under https://lightsources.org, (accessed 7 November 2022).
[20] A. S. Ditter, E. P. Jahrman, L. R. Bradshaw, X. Xia, P. J. Pauzauskie, G. T. Seidler, *J. Synchrotron Radiat.* **2019**, *26*, 2086–2093.
[21] P. Zimmermann, S. Peredkov, P. M. Abdala, S. DeBeer, M. Tromp, C. Müller, J. A. van Bokhoven, *Coord. Chem. Rev.* **2020**, *423*, 213466.
[22] W. Błachucki, J. Czapla-Masztafiak, J. Sá, J. Szlachetko, *J. Anal. At. Spectrom.* **2019**, *34*, 1409–1415.
[23] Z. Németh, J. Szlachetko, É. G. Bajnóczi, G. Vankó, *Rev. Sci. Instrum.* **2016**, *87*, 103105.
[24] W. Malzer, C. Schlesiger, B. Kanngießer, *Spectrochim. Acta Part B* **2021**, *177*, 106101.
[25] G. T. Seidler, D. R. Mortensen, A. J. Remesnik, J. I. Pacold, N. A. Ball, N. Barry, M. Styczinski, O. R. Hoidn, *Rev. Sci. Instrum.* **2014**, *85*, 113906.
[26] A. P. Honkanen, S. Ollikkala, T. Ahopelto, A. J. Kallio, M. Blomberg, S. Huotari, *Rev. Sci. Instrum.* **2019**, *90*, 033107.
[27] R. Bès, T. Ahopelto, A. P. Honkanen, S. Huotari, G. Leinders, J. Pakarinen, K. Kvashnina, *J. Nucl. Mater.* **2018**, *507*, 50–53.
[28] C. Schlesiger, S. Praetz, R. Gnewkow, W. Malzer, B. Kanngießer, *J. Anal. At. Spectrom.* **2020**, *35*, 2298–2304.
[29] N. S. Genz, A–J Kallio, R. Oord, F. Krumeich, A. Pokle, Ø. Prytz, U. Olsbye, F. Meirer, S. Huotari, B. M. Weckhuysen, *Angew. Chem. Int. Ed.* **2022**, e202209334.
[30] J. G. Moya-Cancino, A. P. Honkanen, A. M. J. van der Eerden, H. Schaink, L. Folkertsma, M. Ghiasi, A. Longo, F. M. F. de Groot, F. Meirer, S. Huotari, B. M. Weckhuysen, *ChemCatChem* **2019**, *11*, 1039–1044.
[31] J. G. Moya-Cancino, A. P. Honkanen, A. M. J. van der Eerden, H. Schaink, L. Folkertsma, M. Ghiasi, A. Longo, F. Meirer, F. M. F. de Groot, S. Huotari, B. M. Weckhuysen, *ChemCatChem* **2019**, *11*, 3042–3045.
[32] É. G. Bajnóczi, Z. Németh, G. Vankó, *Inorg. Chem.* **2017**, *56*, 14220–14226.

[33] M. Dimitrakopoulou, X. Huang, J. Kröhnert, D. Teschner, S. Praetz, C. Schlesiger, W. Malzer, C. Janke, E. Schwab, F. Rosowski, H. Kaiser, S. Schunk, R. Schlögl, A. Trunschke, *Faraday Discuss.* **2018**, *208*, 207–225.
[34] W. Bi, J. Wang, E. P. Jahrman, G. T. Seidler, G. Gao, G. Wu, G. Cao, *Small* **2019**, *15*, 1901747.
[35] M. E. Mundy, D. Ung, N. L. Lai, E. P. Jahrman, G. T. Seidler, B. M. Cossairt, *Chem. Mater.* **2018**, *30*, 5373–5379.
[36] W. Bi, E. Jahrman, G. Seidler, J. Wang, G. Gao, G. Wu, M. Atif, M. Alsalhi, G. Cao, *ACS Appl. Mater. Interfaces* **2019**, *11*, 16647–16655.
[37] H. V. Le, S. Parishan, A. Sagaltchik, C. Göbel, C. Schlesiger, W. Malzer, A. Trunschke, R. Schomäcker, A. Thomas, *ACS Catal.* **2017**, *7*, 1403–1412.
[38] P. W. Menezes, C. Walter, J. N. Hausmann, R. Beltrán-Suito, C. Schlesiger, S. Praetz, V. Yu, Verchenko, A. V. Shevelkov, M. Driess, *Angew. Che. Int. Ed.* **2019**, *58*, 16569–16574.
[39] X. Zhao, P. Pachfule, S. Li, T. Langenhahn, M. Ye, C. Schlesiger, S. Praetz, J. Schmidt, A. Thomas, *J. Am. Chem. Soc.* **2019**, *141*, 6623–6630.
[40] R. L. Oliveira, M. C. Ben Ghorbel, S. Praetz, D. Meiling, C. Schlesiger, R. Schomäcker, A. Thomas, *ACS Sustainable Chem. Eng.* **2020**, *8*, 11171–11182.
[41] J. K. Lee, Y. J. Kim, H. J. Lee, S. H. Kim, S. J. Cho, I. S. Nam, S. B. Hong, *J. Catal.* **2011**, *284*, 23–33.
[42] T. Yamamoto, A. Teramachi, A. Orita, A. Kurimoto, T. Motoi, T. Tanaka, *J. Phys. Chem. C* **2016**, *120*, 19705–19713.
[43] W. Wang, L. Kuai, W. Cao, M. Huttula, S. Ollikkala, T. Ahopelto, A.-P. Honkanen, S. Huotari, M. Yu, B. Geng, *Angew. Chem. Int. Ed.* **2017**, *129*, 15173–15177.
[44] W. Bi, J. Huang, M. Wang, E. P. Jahrman, G. T. Seidler, J. Wang, Y. Wu, G. Gao, G. Wu, G. Cao, *J. Mater. Chem. A* **2019**, *7*, 17966–17973.
[45] E. P. Jahrman, L. A. Pellerin, A. S. Ditter, L. R. Bradshaw, T. T. Fister, B. J. Polzin, S. E. Trask, A. R. Dunlop, G. T. Seidler, *J. Electrochem. Soc.* **2019**, *166*, 2549–2555.
[46] B. M. Weckhuysen, *Phys. Chem. Chem. Phys.* **2003**, *5*, 4351–4360.
[47] I. L. C. Buurmans, B. M. Weckhuysen, *Nat. Chem.* **2012**, *4*, 873–886.
[48] M. A. Bañares, *Adv. Mater.* **2011**, *23*, 5293–5301.
[49] U. Bentrup, *Chem. Soc. Rev.* **2010**, *39*, 4718–4730.
[50] B. M. Weckhuysen, *Angew. Chem. Int. Ed.* **2009**, *48*, 4910–4943.
[51] T. Taguchi, J. Harada, A. Kiku, K. Tohji, K. Shinoda, *J. Synchrotron Radiat.* **2001**, *8*, 363–365.
[52] C. Schlesiger, L. Anklamm, H. Stiel, W. Malzer, B. Kanngießer, *J. Anal. At. Spectrom.* **2015**, *30*, 1080–1085.
[53] Y. N. Yuryev, H. J. Lee, H. M. Park, Y. K. Cho, M. K. Lee, K. J. Pogrebitsky, *Rev. Sci. Instrum.* **2007**, *78*, 025108.
[54] J. Timoshenko, A. Shivhare, R. W. J. Scott, D. Lu, A. I. Frenkel, *Phys. Chem. Chem. Phys.* **2016**, *18*, 19621–19630.
[55] J. Timoshenko, D. Lu, Y. Lin, A. I. Frenkel, *J. Phys. Chem. Lett.* **2017**, *8*, 5091–5098.
[56] Y. Liu, N. Marcella, J. Timoshenko, A. Halder, B. Yang, L. Kolipaka, M. J. Pellin, S. Seifert, S. Vajda, P. Liu, A. I. Frenkel, *J. Chem. Phys.* **2019**, *151*, 164201.
[57] N. Marcella, Y. Liu, J. Timoshenko, E. Guan, M. Luneau, T. Shirman, A. M. Plonka, J. E. S. Van Der Hoeven, J. Aizenberg, C. M. Friend, A. I. Frenkel, *Phys. Chem. Chem. Phys.* **2020**, *22*, 18902–18910.
[58] O. Müller, M. Nachtegaal, J. Just, D. Lützenkirchen-Hecht, R. Frahm, *J. Synchrotron Radiat.* **2016**, *23*, 260–266.
[59] S. R. Bare, A. Boubnov, J. Hong, A. S. Hoffman, *Synchrotron Radiat. News* **2020**, *33*, 15–19.
[60] A. Longo, C. J. Sahle, P. Glatzel, C. Giacobbe, A. Rack, O. Mathon, K. A. Lomachenko, J. Segura-Ruiz, J. Villanova, H. Castillo-Michel, V. Vanpeene, R. Tucoulou, T. U. Schülli, I. Martens, J. Drnec, *Synchrotron Radiat. News* **2020**, *33*, 40–51.
[61] W. A. Caliebe, V. Murzin, A. Kalinko, M. Görlitz, *AIP Conf. Proc.* **2019**, *2054*, 060031.
[62] A.-J. Kallio, A. Weiß, R. Bes, M. Heikkilä, M. Ritala, M. Kemell, S. Huotari, *Dalton Trans.* **2022**, *51*, 18593.
[63] M. Bauer, *Phys. Chem. Chem. Phys.* **2014**, *16*, 13827–13837.
[64] T. Gog, D. M. Casa, A. H. Said, M. H. Upton, J. Kim, I. Kuzmenko, X. Huang, R. Khachatryan, *J. Synchrotron Radiat.* **2013**, *20*, 74–79.
[65] M. Rovezzi, C. Lapras, A. Manceau, P. Glatzel, R. Verbeni, *Rev. Sci. Instrum.* **2017**, *88*, 013108.
[66] R. K. T. Gog, D. Casa, A. Said, M. Upton, Jung Ho Kim, I. Kuzmenko, X. Huang, "Near-Backscattering, Spherical Analyzers for RIXS: A Compilation of Viable Reflections in Si, Ge, LiNbO3, Sapphire and Quartz," can be found under https://www.aps.anl.gov/Analyzer-Atlas/Analyzer-Atlas, (accessed 7 November 2022).
[67] A. J. Achkar, T. Z. Regier, H. Wadati, Y. J. Kim, H. Zhang, D. G. Hawthorn, *Phys. Rev. B: Condens. Matter Mater. Phys.* **2011**, *83*, 2–5.
[68] R. Kurian, K. Kunnus, P. Wernet, S. M. Butorin, P. Glatzel, F. M. F. De Groot, *J. Phys. Condens. Matter* **2012**, *24*, 452201.
[69] T. Poikela, J. Plosila, T. Westerlund, M. Campbell, M. De Gaspari, X. Llopart, V. Gromov, R. Kluit, M. Van Beuzekom, F. Zappon, V. Zivkovic, C. Brezina, K. Desch, Y. Fu, A. Kruth, *J. Instrum.* **2014**, *9*, C05013.
[70] K. D. Bartle, P. Myers, *TrAC Trends Anal. Chem.* **2002**, *21*, 547–557.
[71] K. Dettmer-Wilde, W. Engewald, *Practical Gas Chromatography*, Springer, Heidelberg, **2014**.
[72] G. L. Glish, R. W. Vachet, *Nat. Rev. Drug Discovery* **2003**, *2*, 140–150.
[73] J. H. Gross, *Mass Spectrometry*, Springer, Heidelberg, **2011**.
[74] "XANES Analysis: Linear Combination Analysis, Principal Component Analysis, Pre-edge Peak Fitting," can be found under https://cars.uchicago.edu/xraylarch/xafs/xanes.html, (accessed 25 July 2023).
[75] A. Kuzmin, J. Chaboy, *IUCrJ* **2014**, *1*, 571–589.
[76] C. Piquer, M. A. Laguna-Marco, A. G. Roca, R. Boada, C. Guglieri, J. Chaboy, *J. Phys. Chem. C* **2014**, *118*, 1332–1346.
[77] J. Nilsson, P. A. Carlsson, H. Grönbeck, M. Skoglundh, *Top. Catal.* **2017**, *60*, 283–288.
[78] D. R. Mortensen, G. T. Seidler, *J. Electron Spectrosc. Relat. Phenom.* **2017**, *215*, 56–61.
[79] M. Bitter, K. W. Hill, S. Scott, R. Feder, J. Ko, A. Ince-Cushman, J. E. Rice, *Rev. Sci. Instrum.* **2008**, *79*, 10E927.
[80] "XAS Powder Sample Weight Calculator," can be found under https://www-ssrl.slac.stanford.edu/smbin/mucalwebnew.pl, (accessed 7 November 2022).
[81] B. Ravel, M. Newville, *J. Synchrotron Radiat.* **2005**, *12*, 537–541.
[82] K. Klementiev, *J. Phys. Conf. Ser.* **2016**, *712*, 012008.
[83] E. A. Stern, K. Kim, *Phys. Rev. B* **1981**, *23*, 3781–3787.
[84] N. Fischer, B. Clapham, T. Feltes, E. Van Steen, M. Claeys, *Angew. Chem. Int. Ed.* **2014**, *53*, 1342–1345.
[85] A. J. Foster, R. F. Lobo, *Chem. Soc. Rev.* **2010**, *39*, 4783–4793.

Manuscript received: May 6, 2023
Version of record online: August 17, 2023